Vegetable Research

ARTICLE

Open Access

https://doi.org/10.48130/vegres-0025-0032

Vegetable Research **2025**, 5: e038

SlRLK55 negatively regulates phosphate starvation response in tomato

Yakun Wang[1,2#], Yunfeng Zhao[1,3#], Mingtong Zhai[1,3#], Yibo Wang[1,2#], Huawei Zhai[1,2], Xianwen Meng[1,2], Qian Chen[1,4*] and Chuanyou Li[1,5*]

[1] *Taishan Academy of Tomato Innovation, Shandong Agricultural University, Tai'an 271018, Shandong, China*
[2] *College of Horticulture Science and Engineering, Shandong Agricultural University, Tai'an 271018, Shandong, China*
[3] *College of Agronomy, Shandong Agricultural University, Tai'an 271018, Shandong, China*
[4] *Beijing Key Laboratory for Agricultural Applications and New Techniques, Plant Science and Technology College, Beijing University of Agriculture, Beijing 102206, China*
[5] *College of Life Science, Shandong Agricultural University, Tai'an 271018, Shandong, China*
[#] Authors contributed equally: Yakun Wang, Yunfeng Zhao, Mingtong Zhai, Yibo Wang
* Corresponding authors, E-mail: chenqiangenetics@163.com; cyli@genetics.ac.cn

Abstract

Phosphate (Pi) deficiency is a major abiotic stress factor limiting plant growth and development. The underlying mechanism of how plants uptake and use Pi with high efficiency is relatively unexplored in *Solanum lycopersicum*. In this study, we focus on the function of *receptor-like kinase 55* of *Solanum lycopersicum* (*SlRLK55*) in regulating phosphate starvation response (PSR). Our genetic data found that *SlRLK55* is a negative modulator of PSR. In-depth study demonstrates that *SlRLK55* plays negative roles in regulating PSR gene expression, root growth, organic acid secretion, and phosphatase activities against phosphate deprivation. Based on our genetic and physiological data, it is concluded that *SlRLK55* is an important negative regulator of PSR in tomato.

Citation: Wang Y, Zhao Y, Zhai M, Wang Y, Zhai H, et al. 2025. *SlRLK55* negatively regulates phosphate starvation response in tomato. *Vegetable Research* 5: e038 https://doi.org/10.48130/vegres-0025-0032

Introduction

Phosphorous (P) is one of the pivotal nutrients for crop quality and quantity[1]. Inorganic phosphate (Pi) is the primary form of P that can be absorbed by plants from soil. The most remarkable feature of Pi is its low availability and mobility in soil caused by Fe^{3+} and Al^{3+} at acid pH and calcium at alkaline pH[2]. Only a small fraction of Pi fertilizer is available to plants, with the majority being immobilized in the soil. This leads to the low efficiency of Pi absorbed by crops. To deal with this, excess fertilizer is used in modern agriculture, which leads to environmental pollution[3]. Most significantly, the finite reserves of rock phosphate are predicted to be fully depleted by the end of this century[4]. In-depth understanding of the molecular mechanism of phosphate uptake and utilization contributes to breeding for high-nutrient-efficiency crops, thus reducing over-reliance on phosphate fertilizers.

To cope with Pi limitation, plants developed a distinct mechanism of Pi starvation response (PSR) to enhance the use efficiency[5,6]. To enhance the ability to acquire Pi from soil, the root system architecture is modified. This modification involves increasing the density of lateral roots and root hairs while simultaneously inhibiting primary root elongation. These adaptations enable plants to more effectively explore the topsoil for phosphate and significantly expand the root-soil interface, thereby enhancing their overall capacity to absorb Pi[7,8]. Plant roots also secret organic acids, nucleases, and phosphatase to release Pi from insoluble or organic materials[9]. The phosphate starvation response (PSR) further promotes the interaction of plant roots with beneficial soil-borne microorganisms, serving as an important strategy for plants to obtain phosphate from the soil[10–12]. When plants encounter Pi deficiency, transcriptional reprogramming takes place to modulate Pi signaling and homeostasis[13,14]. PHOSPHATE STARVATION RESPONSE1 (AtPHR1) in *Arabidopsis* and its homologues in other plants, are the hub of transcriptional reprograming during PSR[15].

In Pi-deficient conditions, PHR1 directly regulates PSR genes transcription, such as Pi transporter and microRNAs[14]. SPX domain-containing proteins (SPXs) serve as transcriptional repressors of PHRs by attenuates dimerization, DNA binding activities, and protein localization of PHR proteins[16]. Through the SPX-PHR interaction, these proteins function as phosphate (Pi) sensors[17]. SPX proteins bind inositol polyphosphate (InsP) and inositol pyrophosphate (PP-InsP) rather than Pi *in vitro*, and the binding of SPX1 with InsP/PP-InsP facilitates the interaction between OsSPX1 and OsPHR2[16]. This imply that InsP/PP-InsP are the components representing intracellular Pi status, which affects SPX1/2-PHR1 interaction. Under normal conditions, SPX1/2 proteins serve as repressors by preventing PHR1 binding PSR promoters, and SPX4 prevents PHR1 from entering the nucleus in *Arabidopsis*. Pi deprivation promotes the dissociation of SPX1/2 from the PHR1-SPX complex in the nucleus, while the dissociation of SPX4 from the SPX4-PHR1 complex facilitates the translocation of PHR1 from the cytoplasm to the nucleus, thereby activating the PSR[18,19]. To avoid the over-activation of PSR, the E3 ligase, NITROGEN LIMITATION ADAPTATION (NLA), polyubiquitinates and degrades PHR1 in *Arabidopsis*[20]. PHR proteins also serve as the central hub in arbuscular mycorrhizal symbiosis-mediated phosphate (Pi) uptake from the soil[11,12].

Receptor-like protein kinases (RLKs) constitute a distinct class of transmembrane proteins that are abundant in plants. These proteins play a pivotal role in perceiving and transducing extracellular signals, thereby orchestrating diverse processes including plant growth, development, and stress responses[21,22]. Inositol Polyphosphate-related Cytoplasmic Kinases 1–6 (IPCK1–IPCK6) are intricately involved in the accumulation of InsP6, which constitutes the primary form of Pi in seeds[23]. Proline-rich extensin-like receptor kinase 13 (PERK13) contributes to phosphate (Pi) deficiency-induced root hair growth, likely by modulating root hair elongation, and reactive oxygen species (ROS) generation[24]. While significant progress has

been made in elucidating the mechanisms by which RLKs sense abiotic and biotic stress signals, our knowledge in understanding how RLKs regulate PSR is still far behind. Identifying the RLKs involved in PSR will enrich our understanding of how plants transduce environmental cues into cellular response.

Tomato is an important vegetable crop. The PHRs-SPXs-mediated PSR in tomato has recently been clarified[12,15,25]. However, the mechanism by which PSR is regulated in tomato remains poorly understood. In this study, we focus on the function of *receptor-like kinase 55* of tomato (*SlRLK55*) in regulating PSR. Our genetic data found that *SlRLK55* is a negative modulator of PSR. In-depth study demonstrates that *SlRLK55* plays important roles in regulating PSR gene expression, root growth, organic acid secretion, and phosphatase activities against phosphate deprivation. All these illustrate that *SlRLK55* is an important negative regulator of PSR in tomato.

Materials and methods

Plant materials and growth conditions

The wild-type tomato used in this study was M82. The *slrlk55-cr* mutant was created by CRISPR/Cas9 gene editing technology in the M82 background. Tomato plants were grown in a greenhouse in Tai'an, Shandong Province (China), for subsequent phenotyping.

The germinated seeds were grown on 1/2 MS medium. When the first true leaves appeared, the seedlings with uniform growth were picked out and transplanted into vermiculite, watered with 500 mL pure water, and then watered two days later using Pi deprivation nutrient solution, which was repeated at intervals of 3–4 d. The nutrient solution contains 2.1 M NH_4NO_3, 1.9 M KNO_3, 1 M $Ca(NO_3)_2$, 0.3 M $CaCl_2$, 0.15 M $MgSO_4$, 100 mM $FeSO_4$, 100 mM H_3BO_3, 100 mM $MnSO_4$, 30 mM $ZnSO_4$, 1 mM $CuSO_4$, 1 mM $NaMoO_4$, and 1 M KH_2PO_4. Phosphate-sufficient nutrient solution contains 1 mM KH_2PO_4, and phosphate-limited nutrient solution contains 50 μM KH_2PO_4. Tomato seedlings were grown at 28 °C for 16 h of light, 22 °C for 8 h of darkness, and 40% relative humidity. Photographs were taken after three weeks of Pi deprivation treatment, and measurements were taken.

SlRLK55 sequence assessment

The SlRLK55 sequence alignment was carried out using DNAMAN (v8.0)[26]. Protein structural domains of SlRLK55 were predicted using NCBI (www.ncbi.nlm.nih.gov). The transmembrane domains of SlRLK55 were predicted using the TMHMM algorithm. Phylogenetic analysis was performed using MEGA 11 based on a neighbor-joining method with 1,000 bootstrap replicates and removal of bootstrap scores less than 50%.

RNA extraction and gene expression analysis

Total RNA was extracted from different tissues of tomato using Trizol reagent (TransGen Biotech, Beijing, China), and the resulting RNA was used for first strand cDNA synthesis by the TransScript® Uni All-in-One kit (TransGen Biotech, Beijing, China) according to the manufacturer's instructions. The gene expression levels were analysed by qRT-PCR using the CFX96 Real-Time PCR System (BIORAD, USA), and the assay was performed according to the method described previously[27]. *SlACTIN* was used as an internal reference. Expression analysis was carried out in accordance with a previous method[28]. Primers were listed in Supplementary Table S1.

CRISPR/Cas9-mediated mutations

The *slrlk55-cr* mutant was created in the M82 background by CRISPR/Cas9 as described in previous studies[27,29,30]. Targets were predicted using the CRISPR Direct target design website. *PTX043* was used as a template, and the target sequence was amplified using TransStrart FastPfu Fly DNA Polymerase reagent referring to the product instructions. The target sequence was cloned into the *PTX041* vector with the BsaI restriction site. The construct was transformed into the *Agrobacterium* strain (LBA4404) and subsequently transformed into M82 by *Agrobacterium*-mediated cotyledon explant transformation. The transgenic plants were identified by PCR amplification and DNA sequencing. Homozygous *slrlk55-cr* transgenic plants obtained in the T_2 generation were used for further experiments. Primers were listed in Supplementary Table S1.

Subcellular localization assay

The coding sequence of *SlRLK55* was cloned into the *pK7FWG2*[31] vector with EcoRI and XhoII restriction sites to generate the *35S:SlRLK55*-GFP construct. *35S:SlRLK55-GFP* and a plasma membrane marker (pm-rk) were co-transformed into *N. benthamiana* leaves. Fluorescence signals were detected using an ultra-high resolution laser confocal microscope (LSM880). Primers were listed in Supplementary Table S1.

Anthocyanin determination

According to a previous study[8] with minor modifications[32]. Seedling samples (0.1 g) were placed in 300 μL of 0.1% HCl methanol solution in a refrigerator at −4 °C for 4 h. Two hundred μL of distilled water and 500 μL of chloroform were added and mixed with shaking, and then centrifuged at 13,000 rpm for 5 min, the supernatant was measured for absorbance at A_{530} and A_{657} to determine the total amount of anthocyanins in the aqueous phase.

$$\text{Anthocyanin content } (OD_{530-657}\ g^{-1}) = (OD_{530} - OD_{657})/0.1\ g$$

where, OD_{530}: absorbance value at 530 nm. OD_{657}: absorbance value at 657 nm.

Phosphate content determination

According to a previous study[33], Pi content was determined with M82, *slrlk55-cr-1*, and *slrlk55-cr-2* samples grown under control and Pi deprivation conditions. Pi content was measured at A_{820}.

Root system architecture analysis

Germinated M82 and *slrlk55-cr* seeds were directly grown on 1/2 MS medium with Pi sufficiency or Pi deprivation, and grown at 28 °C for 16 h of light and 22 °C for 8 h of darkness. To observe the root growth of tomato seedlings, plates with seedlings were scanned using an Epson Perfection V800 scanner at 600 dpi. The length of primary roots and the number of lateral roots were quantified using ImageJ software (https://imagej.nih.gov/ij/). After measuring root morphology, roots were used for acid phosphatase determination.

Determination of acid phosphatase activity

Acid phosphatase activity was measured in seedling roots treated with Pi deprivation for 5 d using an ACP activity kit (Elabscience, Huston, TX, USA) following the product instructions. Protein concentration was measured using the BCA Protein Concentration Kit (Elabscience, Huston, TX, USA). Absorbance at 405 nm was measured using a Tecan Infinite 200 enzyme labeler (Tecan, Männedorf, Switzerland).

BCP staining

According to a previous study with minor modifications[34]. Bromocresol violet (color changed from yellow at pH 5.2 to purple at pH = 6.8) was added to 1/2 MS medium with Pi deprivation to form an agar-indicator mixture. Seedlings with root length about 4 cm were transferred to 1/2 MS medium containing bromocresol violet with Pi deprivation for the indicated time points. The plants were photographed and counted according to the color response of the roots.

Results

Bioinformatics analysis of *SlRLK55*

SlRLK55 (Solyc03g124050) encodes 713 amino acids. The RLK55 protein sequences from *Solanum lycopersicum* and other plants were compared by DNAMAN software. SlRLK55 showed high similarity with its homologues (Fig. 1a). Phylogenetic tree was established with RLK55 sequences from 12 species by MEGA 11 software. SlRLK55 and its counterparts from *Solanum pennellii* and *Solanum tuberosum* clustered together, which suggests that SlRLK55 is evolutionarily conserved in plants (Fig. 1b). Leucine-rich repeat (LRR) domains and kinase domain exist in the N-terminus and C-terminus of SlRLK55, respectively (Fig. 1c). Transmembrane domains localize in the central part of SlRLK55 (Supplementary Fig. S1). The conserved motif analysis suggests that SlRLK55 is a classic LRR-RLK.

Subcellular localization of SlRLK55

To determine the localization of SlRLK55, *SlRLK55* was amplified from tomato seedlings and cloned into pK7FWG2 with a green fluorescent protein (GFP) tag (Fig. 2a). *35S:SlRLK55-GFP* and mCherry-labeled plasma membrane marker (pm-rk) were co-transformed into *N. benthamiana* leaves by transient expression assays. GFP fluorescence of SlRLK55-GFP was visualized on the cell membrane, which overlapped with the red fluorescence of mCherry (Fig. 2b). The results indicate that SlRLK55 is localized in the cell membrane.

Transcription of *SlRLK55* is induced by phosphate deprivation

The expression pattern of *SlRLK55* was checked in various organs in the cultivar M82 by quantitative reverse transcription PCR (qRT-PCR). *SlRLK55* was expressed in all examined organs, with maximal expression level in flower, moderate level in root and leaf, and lower level in stem and fruit (Fig. 3a). To verify whether *SlRLK55* expression is induced by phosphate (Pi) deprivation, the M82 seedlings treated without and with Pi deprivation were used for qRT-PCR analysis. *SlIPS1* and *SlSPX4* are two of the canonical PSR genes. Upon Pi deprivation, *SlIPS1* exhibited a robust induction, with notable upregulation commencing at the 12-h time point. In contrast, *SlSPX4* was induced at an earlier stage, with detectable expression changes initiated as early as 6 h following the onset of Pi deficiency (Fig. 3b & c). The expression of *SlRLK55* could be strongly induced to a higher level at 24 and 48 h (Fig. 3d). Based on the results, it is concluded that *SlRLK55* expression was induced by Pi deprivation.

SlRLK55 negatively regulates phosphate starvation response in tomato

To clarify whether *SlRLK55* is involved in Pi starvation response (PSR), the *slrlk55-cr* mutant in the cultivar M82 background was constructed by CRISPR/Cas9 gene editing technology. All the mutations in *slrlk55-cr* generated premature stop codons (Supplementary Fig. S2). Plant growth is retarded by Pi deprivation. The plant height was reduced by 41.35%, 32.22%, and 26.84% in M82, *slrlk55-cr-1* and *slrlk55-cr-2* respectively by Pi deprivation (Fig. 4a & b). The fresh weight was also decreased by Pi deprivation by 77.45%, 68.45%, and 67.41% (Fig. 4a & c). The reduction in plant height and fresh weight in *slrlk55-cr* was weaker than that of M82. Anthocyanin accumulation is another hallmark when plants encounter Pi deprivation. Anthocyanin contents were greatly enhanced by Pi deprivation by 551.2%, 376.93%, and 487.97%, in M82, *slrlk55-cr-1,* and *slrlk55-cr-2,* respectively, which illustrates that the PSR-promoted anthocyanin accumulation is significantly lower in *slrlk55-cr* than that of M82 (Fig. 4d). Pi content was diminished by Pi deprivation in M82, but no significant difference was found in *slrlk55-cr* (Fig. 4e). The mutant of *AtRLK55*, a homologue of *SlRLK55* in *Arabidopsis*, also showed reduced root growth inhibition, enhanced root hair elongation and density, and strengthened PSR under Pi deprivation (Supplementary Fig. S3). All these lines of evidence demonstrate that *SlRLK55* is a negative regulator of PSR in tomato.

Root architecture, such as primary root elongation and lateral root density, is modified by Pi deprivation. Under normal conditions, the primary root length of *slrlk55-cr* was slightly but significantly shorter than that of M82. The primary root elongation in M82 was greatly inhibited by Pi deprivation. With Pi deprivation, almost no changes in primary root length were found in *slrlk55-cr* (Fig. 5a & b). Lateral root density and lateral root length were also significantly reduced by Pi deprivation in M82, while the reduction almost disappeared in *slrlk55-cr* (Fig. 5c & d). Pi deprivation promoted root hair elongation and increased root hair density in M82, with this promotional effect being significantly enhanced in *slrlk55-cr* (Fig. 5e–g). These findings indicate that *SlRLK55*-mediated modification of root architecture is involved in plant responses to Pi deprivation.

To further clarify the negative role of *SlRLK55* in PSR, we analysed the expression of several PSR genes, including *SlPT1*, *SlPT3*, *SlPT6*, *SlSPX1*, *SlSPX4,* and *SlIPS1* in M82 and *slrlk55-cr* with Pi deprivation (Fig. 6). All six genes were expressed at similar levels in M82 and *slrlk55-cr* under normal conditions. Pi deprivation could induce these gene expressions in M82, but the induction was enhanced in *slrlk55-cr-1* and *slrlk55-cr-2*.

Taken together, our data demonstrate that *SlRLK55* is a negative regulator of PSR.

Transcription and enzyme activity of phosphatase were repressed by SlRLK55

Increasing phosphatase activity is widely considered as an effective strategy for maximizing Pi uptake[35]. To prove whether phosphatases are involved in *SlRLK55*-mediated PSR, transcription of acid phosphatase genes, such as *SlPAP4*, *SlPAP7*, *SlPAP17,* and *SlPAP26*, was examined with Pi deprivation by qRT-PCR. Under normal conditions, *slrlk55-cr-1* and *slrlk55-cr-2* showed similar transcription levels of *SlPAP4*, *SlPAP7*, *SlPAP17,* and *SlPAP26* compared with that of M82. With Pi deprivation, the transcription was induced in M82, but the induction was stronger in *slrlk55-cr-1* and *slrlk55-cr-2* (Fig. 7a–d). Next, the acid phosphatase (APase) activity was also detected with Pi deprivation in M82 and *slrlk55-cr*. The APase activity was boosted by 32.39%, 81.93%, and 78.98% in M82, *slrlk55-cr-1* and *slrlk55-cr-2* respectively by Pi deprivation, and *slrlk55-cr* showed stronger APase activity compared with that of M82 (Fig. 7e). Based on these, the enhanced transcription and enzyme activity of phosphatase in *slrlk55-cr* could partially account for the reduced sensitivities of *slrlk55-cr* to Pi deprivation.

SlRLK55 modulates organic acid secretion during PSR

When plants encounter Pi deficiency, their roots secrete organic acids into the soil to dissolve Pi from insoluble phosphorus sources, resulting in rhizosphere acidification. The rhizosphere acidification phenotype can be monitored using the pH-indicator dye bromocresol purple (BCP). In 1/2 MS medium supplemented with BCP under Pi deprivation condition, the color changes from purple at pH 6.8 to yellow at pH 5.2[34,36]. On the first day under Pi deprivation conditions, 12%, 44%, and 36% of the seedling roots in M82, *slrlk55-cr-1* and *slrlk55-cr-2*, respectively, turned yellow. On the second and third days, more seedling roots of *slrlk55-cr-1* and *slrlk55-cr-2* turned yellow compared to those of M82 (Fig. 8). These results indicate that the secretion of organic acids under Pi deficiency conditions is negatively regulated by *SlRLK55*.

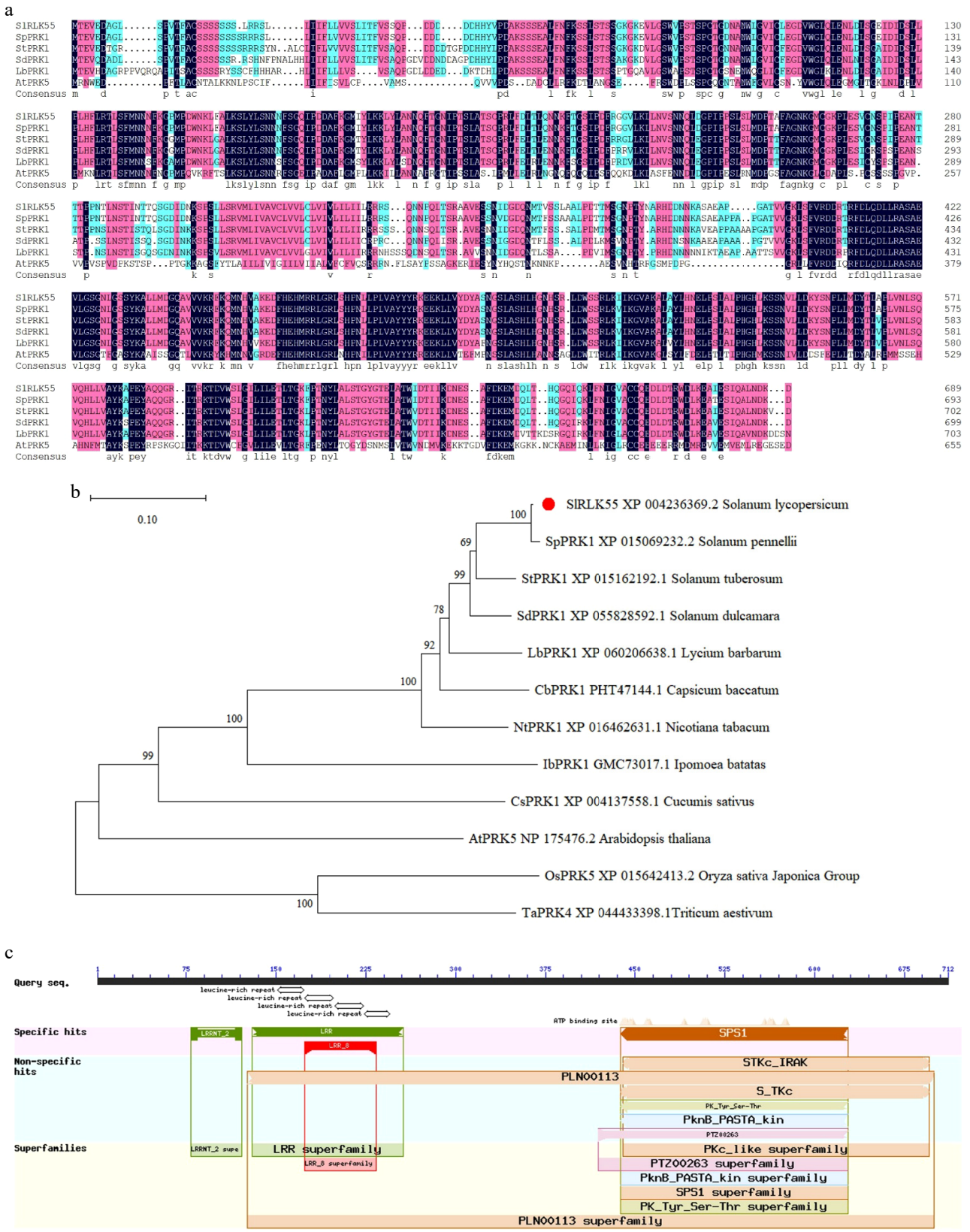

Fig. 1 SlRLK55 sequence analysis. (a) Amino acid sequences comparison of SlRLK55 with potato, bittersweet nightshade, pepper, wolfberry, tobacco, and Arabidopsis. (b) Phylogenetic relationship between SlRLK55 protein and PRK proteins from other plant species. MEGA 11 was used for phylogenetic tree construction with protein sequences from NCBI as follows: *Solanum lycopersicum* (XP_004236369.2); *Solanum pennellii* (XP_015069232.2); *Solanum tuberosum* (XP_015162192.1); *Solanum dulcamara* (XP_055828592.1); *Lycium barbarum* (XP_060206638.1); *Capsicum baccatum* (PHT47144.1); *Nicotiana tabacum* (XP_016480124.1); *Ipomoea batatas* (GMC73017.1); *Cucumis sativus* (XP_004137558.1); *Arabidopsis thaliana* (NP_175476.2); *Oryza sativa* Japonica Group (XP_015642413.2); *Triticum aestivum* (XP_044433398.1). Scales represent branch lengths, and each node represents bootstrap values from 1,000 replicates. (c) Predicted conserved structural domains of SlRLK55.

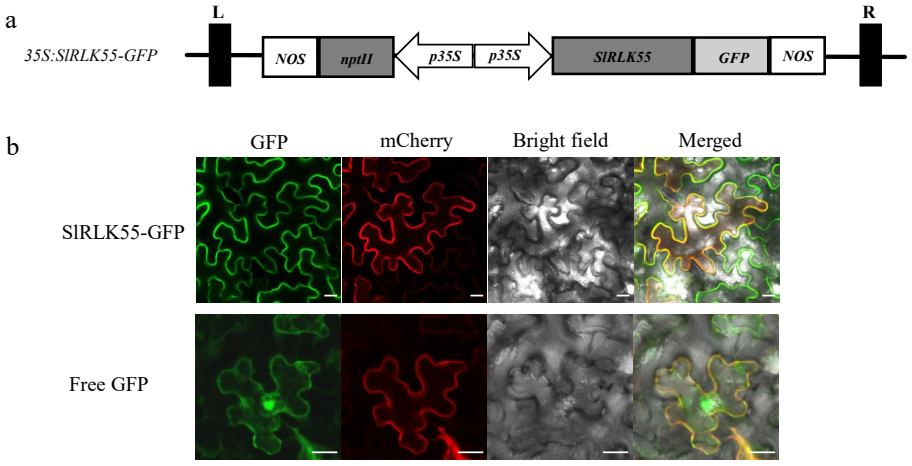

Fig. 2 The subcellular localization of SlRLK55. (a) The *35S:SlRLK55-GFP* plasmid structure. (b) *35S:SlRLK55-GFP* and a mCherry-labeled plasma membrane marker (pm-rk) were co-transformed into *N. benthamiana* leaves by transient expression assay. *35S:GFP* (Free GFP) was used as a control. Green indicates GFP signal. Red indicates the plasma membrane marker (pm-rk) signal. Scale bars = 20 μm.

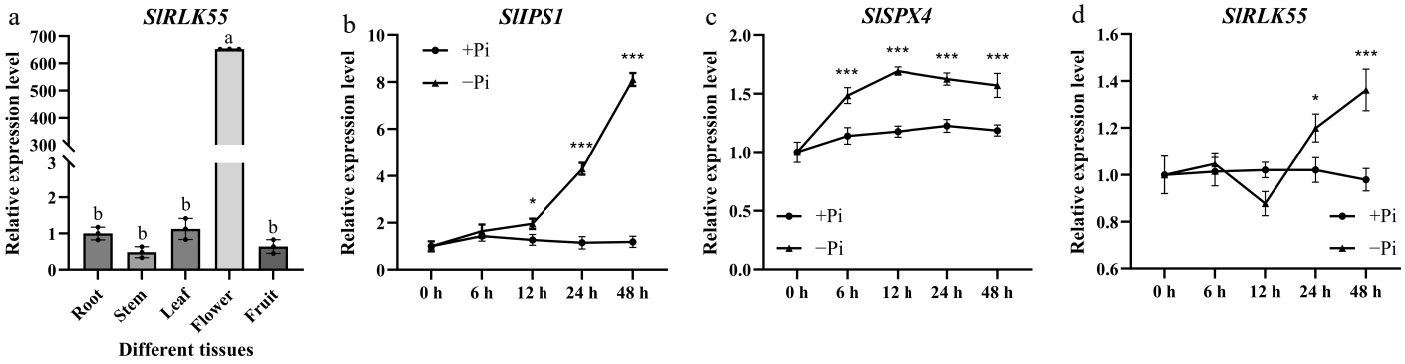

Fig. 3 Assessment of *SlRLK55* expression in M82. (a) Expression of *SlRLK55* was evaluated in roots, stems, leaves, flowers, and fruits of M82. Statistical significance was determined by one-way ANOVA. Significant differences are indicated by different lowercase letters. (b)–(d) Expression of *SlIPS1*, *SlSPX4*, and *SlRLK55* genes in seedlings of M82 treated with Pi deprivation conditions for 0, 6, 12, 24, and 48 h. Three biological replicates of the experiment were performed with similar results. Asterisks denote Student's *t* test significance compared with untreated plants: * $p < 0.05$ and *** $p < 0.001$.

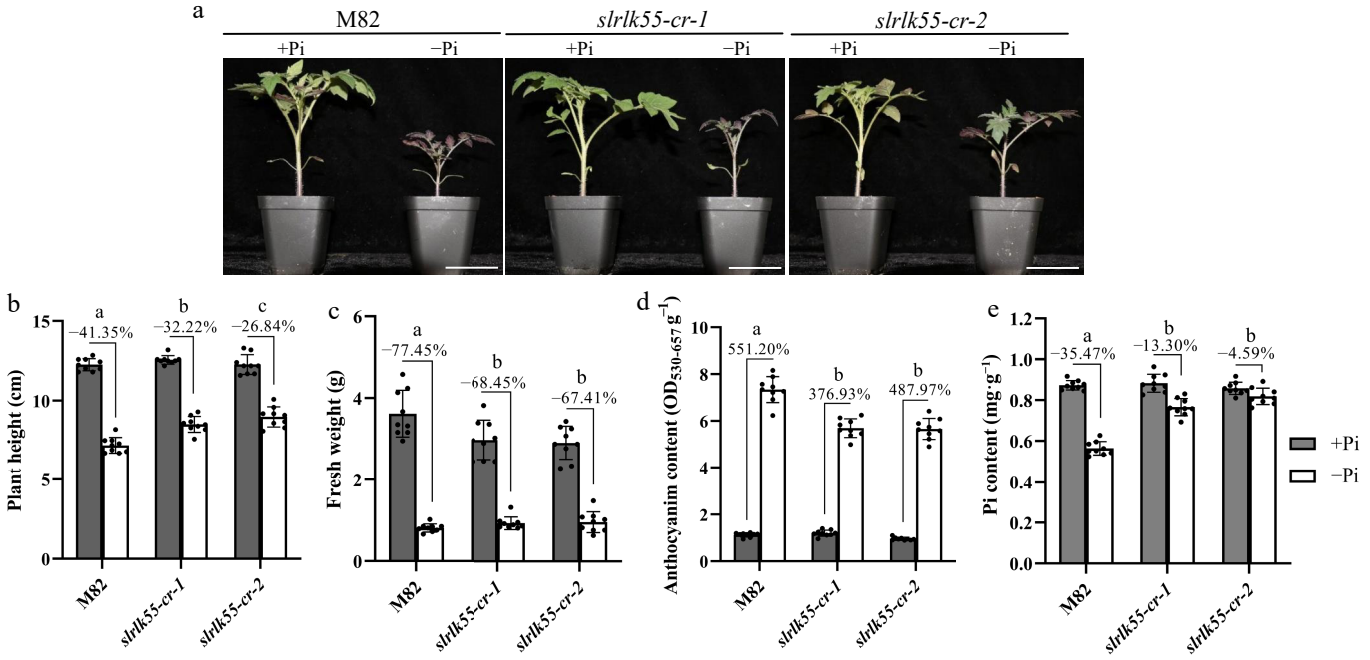

Fig. 4 SlRLK55 is a negative regulator of PSR. (a) Phenotypes of 21-day-old M82 (wild type) and *slrlk55-cr* grown under control (+Pi), and Pi deprivation conditions (−Pi). Seedlings were grown at 28 °C for 16 h of light, 22 °C for 8 h of darkness, and 40% relative humidity. (b) Plant height, (c) fresh weight, (d) anthocyanin content, and (e) Pi content of M82 and *slrlk55-cr* grown in Pi deprivation conditions for 3 weeks. Data are mean ± SD, $n = 3$ repeats. Significant differences are indicated by different lowercase letters. Scale bars = 5 cm.

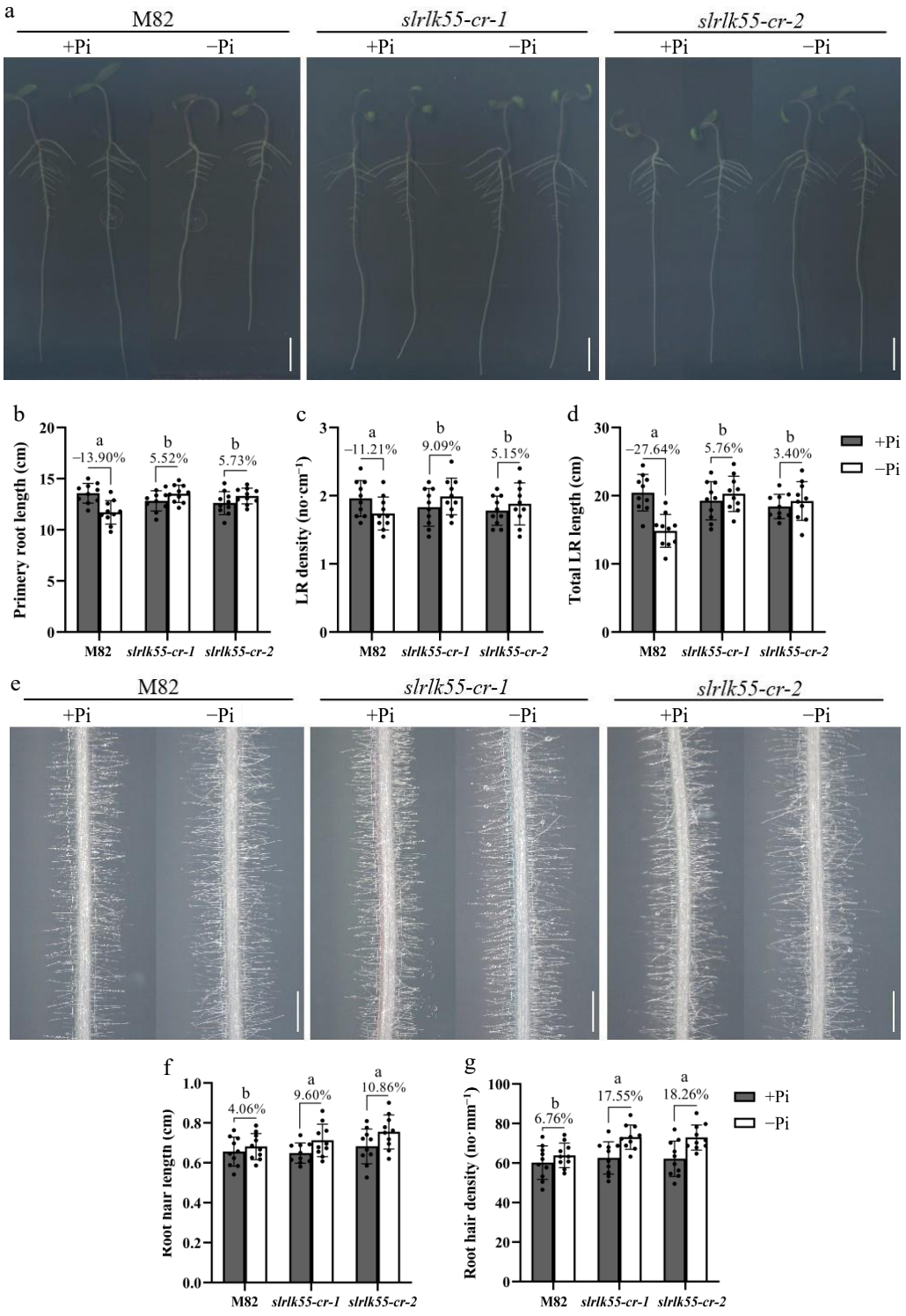

Fig. 5 SlRLK55 negatively affects root architecture under Pi deprivation. (a) Phenotypes of primary root and lateral root (LR) of 7-day-old M82 and *slrlk55-cr* seedlings grown under control (+Pi) and Pi deprivation conditions (–Pi). Bars = 2 cm. (b) Primary root length, (c) lateral root (LR) density, and (d) total LR length of plants shown in (a). (e) Phenotypes of root hairs of 7-day-old M82 and *slrlk55-cr* seedlings grown under control (+Pi) and Pi deprivation conditions (–Pi). Bars = 1 mm. (f) Root hair length, and (g) root hair density of plants shown in (e). Seedlings were germinated on 1/2 MS medium for 2 d and then transferred to 1/2 MS medium with Pi deprivation (–Pi) for another 5 d. Data are mean ± SD, *n* = 3 repeats. Significant differences are indicated by different lowercase letters.

Discussion

Although phosphorous is not deficient in soils, most phosphorous is combined with ions and forms immobile compounds, which limit phosphate absorption by plant roots. To study in-depth the mechanism of high-efficient uptake and usage of Pi, we carried out genetic screening with our receptor-like-kinase (RLK) mutant stock and found *atrlk5-5* showed reduced root growth inhibition by phosphate deficiency (Supplementary Fig. S3). *SlRLK55* is the counterpart of *AtRLK5-5* in tomato. In this study, we focus on the function of

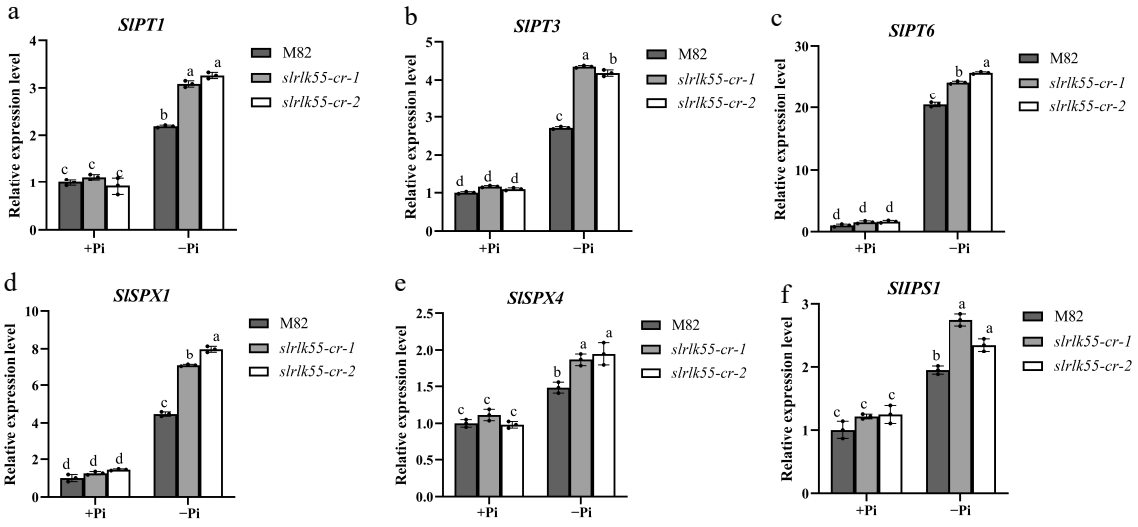

Fig. 6 SlRLK55 exerts a negative effect on the expression of PSR genes. (a)–(f) Expression of PSR genes in seedlings of M82 and *slrlk55-cr* with Pi deprivation treatment (–Pi) for 0 and 48 h. Transcription was analyzed by RT-qPCR with *SlACTIN* as the internal reference. Data are mean ± SD, $n = 3$ repeats. Significant differences are indicated by different lowercase letters.

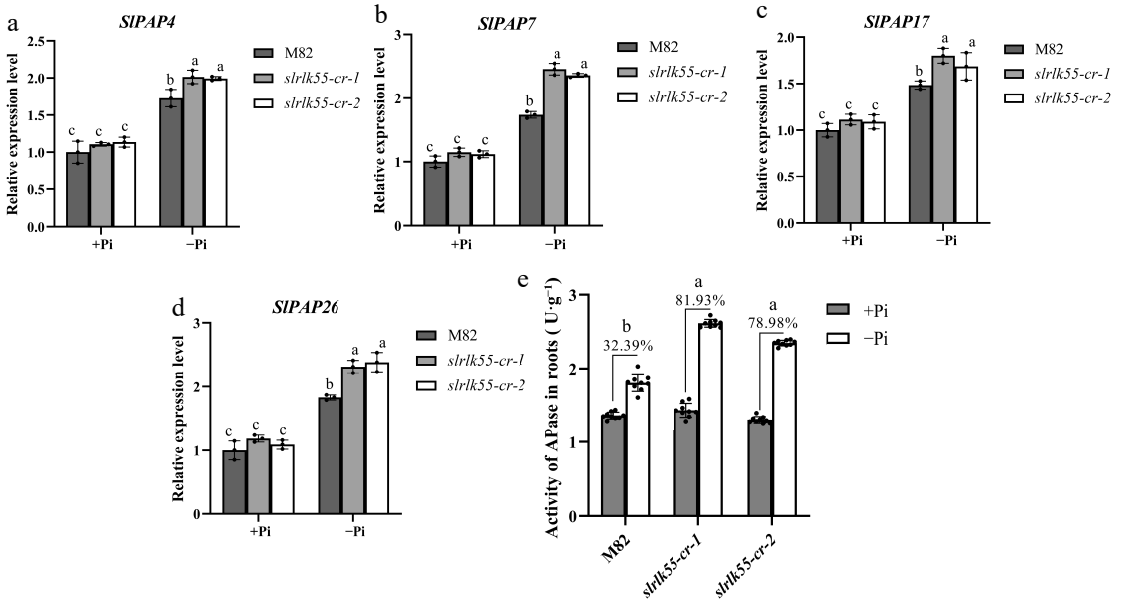

Fig. 7 Transcription and enzyme activity of phosphatase were repressed by SlRLK55. (a)–(d) Expression of acid phosphatase genes in seedlings of M82 and *slrlk55-cr* with Pi deprivation treatment for 0 and 48 h. Transcript levels were analyzed by RT-qPCR with *SlACTIN* as the internal reference gene. (e) Acid phosphatase activity of M82 and *slrlk55-cr*: Two-day-old seedlings grown under control (+Pi) were treated with +Pi and –Pi for another 5 d. Data are mean ± SD, $n = 3$ repeats. Significant differences are indicated by different lowercase letters. (a)–(d) The black bars represent the wild-type M82, while the gray and white bars represent the slrlk55 mutants. (e) The black and white bars represent +Pi and –Pi respectively.

SlRLK55 in the regulation of PSR in tomato. By conserved motif analysis, we found SlRLK55 is a classic LRR-type RLK. SlRLK55 and its counterparts from *Solanum pennellii* and *Solanum tuberosum* clustered together, which suggests that SlRLK55 is evolutionarily conserved in plants (Fig. 1). Subcellular localization assay demonstrates that SlRLK55 is located in cell membrane, which suggests that SlRLK55 is a latent component to transduce extracellular PSR signals into the cytoplasm (Fig. 2).

The subcellular localization of SlRLK55 to the cell membrane further supports its potential role in perceiving environmental cues. The observation that *SlRLK55* transcription is induced by phosphate deprivation suggests a potential feedback mechanism, where the plant upregulates the expression of this negative regulator in response to low phosphate conditions. This induction might be part of a complex regulatory network aiming to fine-tune the PSR, preventing overactivation of phosphate acquisition and utilization pathways.

To genetically test the function of SlRLK55 in PSR, *slrlk55-cr* mutants were constructed by CRISPR/Cas9 gene editing technology. Several physiological indices, such as plant height, fresh weight, anthocyanin contents, Pi contents, primary root elongation, LR density, and LR length were examined with Pi deficiency. Based on the phenotypes analysis, *slrlk55-cr* mutants showed reduced sensitivities to Pi deprivation, which proves the negative role of *SlRLK55* in PSR (Figs 4 & 5). These phenotypic changes suggest that SlRLK55 restricts the plant's adaptive responses to phosphate deficiency, and its absence allows the plant to activate more robust PSR mechanisms.

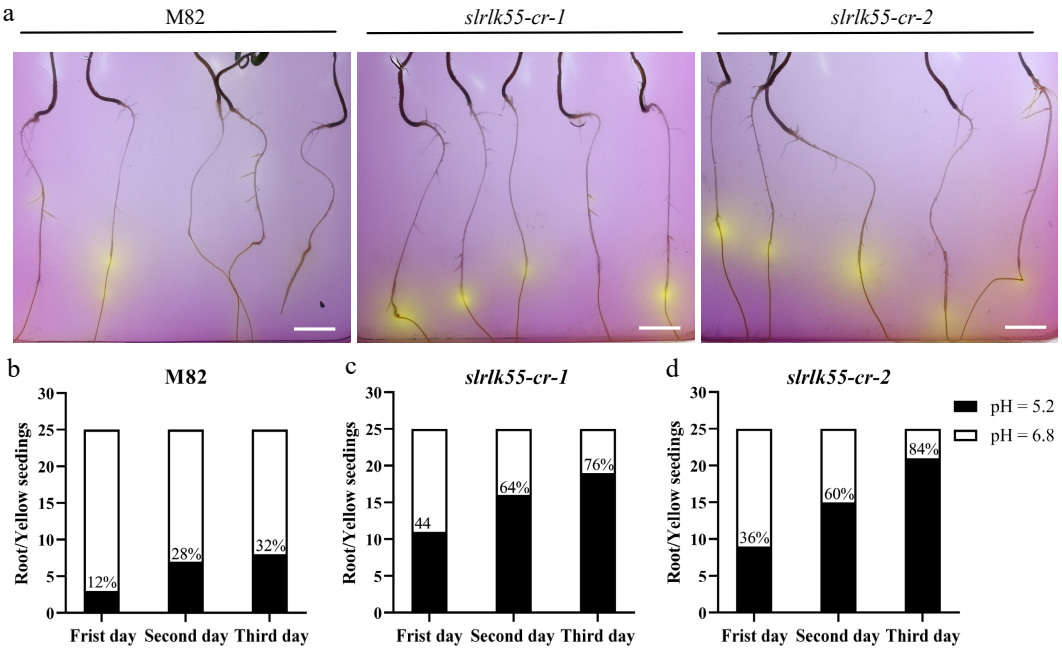

Fig. 8 Organic acid secretion was enhanced in *slrlk55-cr* with Pi deprivation. (a) Root acidification staining of seedlings of M82 and *slrlk55-cr*. Two-day-old seedlings grown with +Pi were transferred to medium containing bromocresol violet with Pi deprivation for another 3 d before the images were taken. The color change from purple to yellow indicates the pH change in the media due to acidification of rhizosphere of plants. Organic acid secretion by the seedling roots of (b) M82, (c) *slrlk55-cr-1*, and (d) *slrlk55-cr-2* after 1 to 3 d growth under Pi deprivation conditions (n = 25). Scale bars = 1 cm.

The analysis of root architecture changes further demonstrated the negative role of *SlRLK55* (Fig. 5). While phosphate deprivation significantly inhibited primary root elongation and reduced LR density and LR length in WT, these inhibitory effects were largely alleviated in *slrlk55-cr*. This indicates that SlRLK55 modulates root architectural adaptations to phosphate availability, potentially by regulating the expression of genes involved in root development and phosphate uptake during PSR.

The expression analysis of PSR-related genes, such as *SlPTs*, *SlSPXs*, and *SlIPS1*, showed that SlRLK55 suppresses their induction by phosphate deprivation (Fig. 6). These genes play crucial roles in phosphate uptake, translocation, and signaling. The enhanced induction of these genes in *slrlk55-cr* suggests that SlRLK55 acts upstream of these components in the PSR pathway, possibly by repressing the activity of transcription factors that activate their expression.

Our study also explored the role of SlRLK55 in regulating phosphatase activity and organic acid secretion during PSR (Figs 7 & 8). Phosphatases are key enzymes involved in phosphate mobilization, and increased phosphatase activity is beneficial for phosphate acquisition from the soil. The *slrlk55-cr* mutant exhibited enhanced transcription of acid phosphatase genes and higher acid phosphatase activity under phosphate-deprived conditions, indicating that SlRLK55 normally represses the expression and activity of phosphatases. Similarly, the increased organic acid secretion in the mutant under phosphate deficiency, as evidenced by the rhizosphere acidification phenotype, suggests that SlRLK55 restricts the release of organic acids, which are important for solubilizing insoluble phosphate sources in the soil.

In conclusion, our study elucidates a novel role for SlRLK55 as a negative regulator of PSR in tomato. SlRLK55 likely functions as a cell surface receptor that senses phosphate availability and suppresses multiple aspects of the plant's adaptive responses to phosphate deficiency, including root architectural changes, PSR gene expression, phosphatase activity, and organic acid secretion. These findings contribute to our understanding of the molecular mechanisms of phosphate homeostasis in plants and may have implications for breeding phosphate-efficient crop varieties. As we did not find the direct interaction of SlRLK55 with SlPHR3, the core component of PSR, and also the transcription factor binding sites of SlPHR3 in *proSlRLK55* (Supplementary Figs S4 & S5), future studies could focus on identifying the upstream signals that activate expression and kinase activity of SlRLK55 and the downstream signaling components that mediate its regulatory effects, further unraveling the complex regulatory network governing PSR.

Author contributions

The authors confirm contributions to the paper as follows: experiments conception and design: Chen Q, Li C; experiment performance: Wang YK, Zhao Y, Zhai M, Wang YB; data analysis: Zhai H, Meng X, Chen Q, Li C; manuscript preparation: Wang YK, Chen Q, Li C. All authors reviewed the results and approved the final version of the manuscript.

Data availability

The datasets produced and/or analyzed throughout this study can be obtained from the corresponding author upon reasonable request.

Acknowledgments

This work was supported by the National Natural Science Foundation of China (32272701 to Qian Chen, 32402596 to Huawei Zhai), Qingdao Municipal Science and Technology Huimin Demonstration Project (23-2-8-xdny-15-nsh to Huawei Zhai and Chuanyou Li), the National Natural Science Foundation of China-Shandong Joint Fund (Grant No. U22A20459 to Chuanyou Li and Qian Chen), the National Key Research and Development Program of China (2022YFD1201700 to Xianwen Meng), and the Agricultural Seed

Project of Shandong Province (2021LZGC017 to Chuanyou Li and Qian Chen).

Conflict of interest

The authors declare that they have no conflict of interest.

Supplementary information accompanies this paper at (https://www.maxapress.com/article/doi/10.48130/tp-0025-0032)

Dates

Received 22 February 2025; Revised 14 July 2025; Accepted 6 August 2025; Published online 20 October 2025

References

1. Puga MI, Poza-Carrión C, Martinez-Hevia I, Perez-Liens L, Paz-Ares J. 2024. Recent advances in research on phosphate starvation signaling in plants. *Journal of Plant Research* 137:315−30
2. Prathap V, Kumar A, Maheshwari C, Tyagi A. 2022. Phosphorus homeostasis: acquisition, sensing, and long-distance signaling in plants. *Molecular Biology Reports* 49:8071−86
3. Heuer S, Gaxiola R, Schilling R, Herrera-Estrella L, López-Arredondo D, et al. 2017. Improving phosphorus use efficiency: a complex trait with emerging opportunities. *The Plant Journal* 90:868−85
4. Xiao X, Zhang J, Satheesh V, Meng F, Gao W, et al. 2022. SHORT-ROOT stabilizes PHOSPHATE1 to regulate phosphate allocation in *Arabidopsis*. *Nature Plants* 8:1074−81
5. Paz-Ares J, Puga MI, Rojas-Triana M, Martinez-Hevia I, Diaz S, et al. 2022. Plant adaptation to low phosphorus availability: core signaling, crosstalks, and applied implications. *Molecular Plant* 15:104−24
6. Li L, Liu KH, Sheen J. 2021. Dynamic nutrient signaling networks in plants. *Annual Review of Cell and Developmental Biology* 37:341−67
7. Gao YQ, Bu LH, Han ML, Wang YL, Li ZY, et al. 2021. Long-distance blue light signalling regulates phosphate deficiency-induced primary root growth inhibition. *Molecular Plant* 14:1539−53
8. Naumann C, Heisters M, Brandt W, Janitza P, Alfs C, et al. 2022. Bacterial-type ferroxidase tunes iron-dependent phosphate sensing during *Arabidopsis* root development. *Current Biology* 32:2189−2205.e6
9. López-Arredondo DL, Leyva-González MA, González-Morales SI, López-Bucio J, Herrera-Estrella L. 2014. Phosphate nutrition: improving low-phosphate tolerance in crops. *Annual Review of Plant Biology* 65:95−123
10. Oldroyd GED, Leyser O. 2020. A plant's diet, surviving in a variable nutrient environment. *Science* 368:eaba0196
11. Shi J, Zhao B, Zheng S, Zhang X, Wang X, et al. 2021. A phosphate starvation response-centered network regulates mycorrhizal symbiosis. *Cell* 184:5527−5540.e18
12. Liao D, Sun C, Liang H, Wang Y, Bian X, et al. 2022. SlSPX1-SlPHR complexes mediate the suppression of arbuscular mycorrhizal symbiosis by phosphate repletion in tomato. *The Plant Cell* 34:4045−65
13. Wang F, Deng M, Xu J, Zhu X, Mao C. 2018. Molecular mechanisms of phosphate transport and signaling in higher plants. *Seminars in Cell & Developmental Biology* 74:114−22
14. Yang SY, Lin WY, Hsiao YM, Chiou TJ. 2024. Milestones in understanding transport, sensing, and signaling of the plant nutrient phosphorus. *The Plant Cell* 36:1504−23
15. Lin D, Tian P, Zhu X, Lin Z, Li Z, et al. 2025. A *PHR* transcription factor-directed gene network reveals key regulators of phosphate metabolism and starvation responses in tomato. *The Plant Cell* 37:koaf171
16. Zhou J, Hu Q, Xiao X, Yao D, Ge S, et al. 2021. Mechanism of phosphate sensing and signaling revealed by rice SPX1-PHR2 complex structure. *Nature Communications* 12:7040
17. Dong J, Ma G, Sui L, Wei M, Satheesh V, et al. 2019. Inositol pyrophosphate $InsP_8$ acts as an intracellular phosphate signal in *Arabidopsis*. *Molecular Plant* 12:1463−73
18. Puga MI, Mateos I, Charukesi R, Wang Z, Franco-Zorrilla JM, et al. 2014. SPX1 is a phosphate-dependent inhibitor of PHOSPHATE STARVATION RESPONSE 1 in *Arabidopsis*. *Proceedings of the National Academy of Sciences of the United States of America* 111:14947−52
19. Lv Q, Zhong Y, Wang Y, Wang Z, Zhang L, et al. 2014. SPX4 negatively regulates phosphate signaling and homeostasis through its interaction with PHR2 in rice. *The Plant Cell* 26:1586−97
20. Park SH, Jeong JS, Huang CH, Park BS, Chua NH. 2023. Inositol polyphosphates-regulated polyubiquitination of PHR1 by NLA E3 ligase during phosphate starvation response in *Arabidopsis*. *New Phytologist* 237:1215−28
21. Escocard de Azevedo Manhães AM, Ortiz-Morea FA, He P, Shan L. 2021. Plant plasma membrane-resident receptors: surveillance for infections and coordination for growth and development. *Journal of Integrative Plant Biology* 63:79−101
22. Dievart A, Gottin C, Périn C, Ranwez V, Chantret N. 2020. Origin and diversity of plant receptor-like kinases. *Annual Review of Plant Biology* 71:131−56
23. Xu LL, Cui MQ, Xu C, Zhang MJ, Li GX, et al. 2024. A clade of receptor-like cytoplasmic kinases and 14-3-3 proteins coordinate inositol hexaphosphate accumulation. *Nature Communications* 15:5107
24. Xue C, Li W, Shen R, Lan P. 2021. *PERK13* modulates phosphate deficiency-induced root hair elongation in *Arabidopsis*. *Plant Science* 312:111060
25. Zhang Y, Wang Y, Wang E, Wu X, Zheng Q, et al. 2021. SlPHL1, a MYB-CC transcription factor identified from tomato, positively regulates the phosphate starvation response. *Physiologia Plantarum* 173:1063−77
26. Guo X, Li J, Zhang L, Zhang Z, He P, et al. 2020. Heterotrimeric G-protein α subunit (LeGPA1) confers cold stress tolerance to processing tomato plants (*Lycopersicon esculentum* Mill). *BMC Plant Biology* 20:394
27. Liu J, Zhang C, Sun H, Zang Y, Meng X, et al. 2024. A natural variation in SlSCaBP8 promoter contributes to the loss of saline–alkaline tolerance during tomato improvement. *Horticulture Research* 11:uhae055
28. Livak KJ, Schmittgen TD. 2001. Analysis of relative gene expression data using real-time quantitative PCR and the $2^{-\Delta\Delta CT}$ method. *Methods* 25:402−8
29. Deng L, Wang H, Sun C, Li Q, Jiang H, et al. 2018. Efficient generation of pink-fruited tomatoes using CRISPR/Cas9 system. *Journal of Genetics and Genomics* 45:51−54
30. Yang T, Ali M, Lin L, Li P, He H, et al. 2023. Recoloring tomato fruit by CRISPR/Cas9-mediated multiplex gene editing. *Horticulture Research* 10:uhac214
31. Karimi M, Inzé D, Depicker A. 2002. GATEWAY™ vectors for *Agrobacterium*-mediated plant transformation. *Trends in Plant Science* 7:193−95
32. He Y, Zhang X, Li L, Sun Z, Li J, et al. 2021. SPX4 interacts with both PHR1 and PAP1 to regulate critical steps in phosphorus-status-dependent anthocyanin biosynthesis. *New Phytologist* 230:205−17
33. Chiou TJ, Aung K, Lin SI, Wu CC, Chiang SF, et al. 2006. Regulation of phosphate homeostasis by microRNA in *Arabidopsis*. *The Plant Cell* 18:412−21
34. Lei KJ, Lin YM, Ren J, Bai L, Miao YC, et al. 2016. Modulation of the Phosphate-Deficient Responses by microRNA156 and its Targeted SQUAMOSA PROMOTER BINDING PROTEIN-LIKE 3 in *Arabidopsis*. *Plant and Cell Physiology* 57:192−203
35. Han M, Chen Y, Li R, Yu M, Fu L, et al. 2022. Root phosphatase activity aligns with the collaboration gradient of the root economics space. *New Phytologist* 234:837−49
36. Yan F, Zhu Y, Müller C, Zörb C, Schubert S. 2002. Adaptation of H^+-pumping and plasma membrane H^+ ATPase activity in proteoid roots of white lupin under phosphate deficiency. *Plant Physiology* 129:50−63